

Adversarial adaptive 1-D convolutional neural networks for bearing fault diagnosis under varying working condition

Bo Zhang^{a,b}, Wei Li^{a,*}, Meng Zhang^a, Zhe Tong^a

^a*School of Mechatronic Engineering, China University of Mining and Technology Xuzhou 221116, Peoples Republic of China*

^b*School of Computer Science And Technology, China University of Mining and Technology Xuzhou 221116, Peoples Republic of China*

Abstract

In recent years, intelligent fault diagnosis algorithms using machine learning technique have achieved much success. However, due to the fact that in real world industrial applications, the working load is changing all the time and the data distributions are different under different working loads, degradation of the performance of intelligent fault diagnosis methods is very serious. In this paper, a new model called A2CNN is proposed to address the problem. Main contributions are concluded: a new domain adaptation method based on adversarial network is proposed in this paper and the method is suitable for processing 1-D Fourier amplitude in fault diagnosis. The transfer learning based on transferring knowledge of parameters is integrated into the train of the proposed model. It can achieve high accuracy when working load is changed. We also visualize the learned features and the networks to try to analyze the reasons behind the high performance of the model.

Keywords: Bearing fault diagnosis, Transfer learning, Domain adaptation, Unsupervised subspace alignment, Vibration signal

1. Introduction

Machine health monitoring is of great importance in modern industry. Failure of these machines could cause great economical loss, and sometimes poses threats to the people who work with the machines. Therefore, in order to keep the industrial machines working properly and reliably, demand for better and more intelligent machine health monitoring technique has never ceased.[1, 2] Rolling element bearings are the most commonly used components in rotating machinery, and bearing faults may result in significant breakdowns, and even casualties.[3, 4] Therefore, effective fault diagnosis plays a highly significant role in increasing the safety and reliability of machinery and preventing possible damage.[5]

In recent years, Deep Learning techniques have achieved huge success in Computer Vision [6, 7] and Speech Recognition[8, 9]. Some deep learning techniques have already found their way into machine health monitoring systems. Jia et al. took the frequency spectra generated by fast Fourier transform (FFT) as the input of stacked autoencoders with three hidden layers for

*Corresponding author. E-mail addresses: liweili_cme@163.com

fault diagnosis of rotary machinery components.[10] Zhu et al. proposed a SAE based DNN for hydraulic pump fault diagnosis that uses frequency features generated by Fourier transform [11]. Liu et al. uses normalized spectrum generated by STFT of sound signal as inputs of a 2-layer SAE based DNN. Some researchers [12, 13] feed multi-domain statistical features including time domain features, frequency domain features and time-frequency domain features into SAE as a way of feature fusion. Recently, there are also some researchers focusing on deep belief network (DBN) with artificer features as inputs.[14] Combination of hierarchical DBN with WPT was found to realize fault location classification.[15] Tao et al. feed deep belief network (DBN) with some time-domain characteristics for fusing multisensor data and fault diagnosis. [16]

Convolutional neural networks (CNN)[17] as one of the most popular deep learning networks is also used to realize fault diagnose the fault of mechanical parts because the weights sharing and spatial pooling. CNN is first proposed by LeCun [18], which have been successfully used in image recognition. Many CNN architectures are proposed, such as VGG-net [19], Res-net [20] and inception v4 [21], for 2-D image recognition. Also, CNN models for 1-D vibration signal were proposed. In [22], the inputs of the CNN model for motor fault detection is 1D raw time vibration signal, which successfully avoids the time-consuming feature extraction process. 1D raw time vibration signal is also taken as the input of CNN by Zhang et al, which realize fault diagnosis under different working load. [23] Guo et al. proposed a hierarchical deep convolution neural network, which consist of functional layers: the first responsible for fault-type recognition and the second responsible for fault-size evaluation. [24] In this paper, frequency spectra is taken as the input of A2CNN, because frequency spectra of rotating machinery show how their constitutive components are distributed with discrete frequencies and may provide clear information about the health conditions of rotating machinery.

For unsupervised learning, most of deep learning techniques, including CNN work well under a common assumption that the labeled training data (source domain) and unlabeled testing data (target domain) are drawn from the same distribution. When the distributions differ, the performances of these approaches may drop dramatically. This situation is called as the cross-domain learning problem. Unfortunately, during the applications of deep learning in bearing fault diagnosis, there are many situations showing disobedience of this assumption, especially when the load condition varies. [25, 26] Domain adaptation (DA) in transfer learning is to solve this kind of problem, which can be introduced into deep learning.[27] DA typically aims at taking full advantage of information coming from both source and target domains during the learning process to adapt automatically. So the key of domain adaptation is how to use the information hidden in target domain. In [26], Lu et al. used the information from normal data in target domain by incorporating maximum mean discrepancy (MMD) into deep neural networks. The MMD regularization term, which measured the discrepancy of normal data in source domain and target domain, is integrated into final objective function. Deep Convolutional Neural Networks with Wide First-layer Kernels (WDCNN) was proposed by zhang [23]. Adaptive batch normalization also combined with WDCNN, which use the mean and variance of target domain to reduce the divergence of distribution between the source domain and target domain. After WDCNN, zhang et. al also proposed a convolution neural networks with training interference (TICNN) model[28]. Compared with WDCNN, dropout was added in the first layers and ensemble learning based on voting was applied.

We can conclude that domain adaptation is to reduce the divergence of distribution between the source domain and target domain, which to some degree is adversarial with the extracted features make data from target domain divisible. So could we find a network to make the data from target domain is discriminative and minimize the divergence of distribution between the

source domain and target domain? In [29], generative adversarial nets is proposed by Goodfellow et. al, which is used to generate the samples. Generative adversarial nets simultaneously train two models, a generative model captures G the data distribution and a discriminative model D estimates the probability that a sample came from the training data rather than G . Inspired by [29], we design a CNN to generate we design a adversarial network based on convolutional neural network, which has strong domain adaptation capacity, named adversarial adaptive 1-D convolutional neural networks (A2CNN). The details of the model will be shown in Section 3. To our best knowledge, this is the first attempt for solving the domain adaptation issues in fault diagnosis by introducing adversarial network. The main contributions of this literature are summarized as follows.

- 1) We proposed a novel network which consists of two networks, normal deep convolutional neural network and deep convolutional adversarial network.
- 2) We introduce transfer learning based on transferring knowledge of parameters into the construction of model during train stage.
- 3) This proposed algorithm has strong domain adaptation capacity, and therefore can achieve high accuracy under different working load.
- 4) We try to explore the inner mechanism of proposed A2CNN model in mechanical feature learning and classification by visualizing the feature maps learned by A2CNN.

The rest of paper is organized as follows. In Section 2, some preliminary knowledge that is used in our proposed framework is briefly reviewed. Section 3 shows the construction of A2CNN. A series of experiments are conducted in Section 4. Finally, the conclusion for this literature is made in Section 5.

2. Preliminary Knowledge

The above CNNs for fault diagnosis mentioned in 1 work well only under a common assumption: The training and test data is drawn from the same distribution. However, vibration signals used for fault diagnosis usually show disobedience of the above assumption. In the running process of rotating machinery, because of complicated working conditions, the distributions of fault data under varying working condition are not consistent. For example, the training samples for building the classifier might be collected under the work condition without the motor load, nevertheless the actual application is to classify the defects from a bearing system under different motor load states. Although the categories of defects remain unchanged, the target data distribution changes with the motor load varies.

Our ultimate goal is to be able to predict labels given a sample from one working condition while the classifier is trained by the samples collected in another working condition. Then, the problem above can be regarded as a domain adaptation problem, which is a realistic and challenging problem in fault diagnosis. To solve this challenge, a domain adaption technique, would be needed to learn a discriminative classifier or other predictor in the presence of a "shift" between training and test distribution by taking full advantage of information coming from both source and target domains.

2.1. Domain Adaptation

According to the survey on domain adaptation for classification [30], a domain \mathcal{D} consists of two components: a feature space \mathcal{X} and a marginal probability distribution P_X , where $X \in \mathcal{X}$. Give a specific domain, a task \mathcal{T} consists of two components: a label space \mathcal{Y} and a prediction

function $f(X)$. From a probabilistic view point, $f(X)$ can be written as the conditional probability distribution $P_{Y|X}$. Given a source domain \mathcal{D}_S and a corresponding learning task \mathcal{T}_S , a target domain \mathcal{D}_T and a corresponding learning task \mathcal{T}_T , domain adaptation aims to improve the learning of the target predictive function f_T in \mathcal{D}_T using the knowledge in \mathcal{D}_S and \mathcal{T}_S , where $\mathcal{D}_S \neq \mathcal{D}_T$ and $\mathcal{T}_S = \mathcal{T}_T$, i.e., the tasks are the same but the domains are different.

In real world applications of fault diagnosis, the working conditions (e.g. motor load and speed) may change from time to time according to the requisite of the production. As a kind of classification problem, the goal of intelligent fault diagnosis is to train classifier with samples collected and labeled in one working condition to be able to classify samples from another working condition. Samples collected under different working conditions can be regarded as different domains. Correspondingly, the fault diagnosis settings in domain adaptation situation are as follows:

- The feature spaces between domains are the same, $\mathcal{X}^S = \mathcal{X}^T$, e.g. the fast Fourier transform (FFT) spectrum amplitudes of raw vibration temporal signals.
- The label spaces between domains are the same, $\mathcal{Y}^S = \mathcal{Y}^T = \{1, \dots, K\}$, where K is the quantity of fault types.
- P_{XY}^S and P_{XY}^T only differ in the marginal probability distribution of the input data, i.e., $P_X^S \neq P_X^T$, while $P_{Y|X}^S = P_{Y|X}^T$.

which is similar to the assumptions in covariate shift [31, 32, 33] or sample selection bias [34].

2.2. Domain Divergence Measure

The main problem existing in domain adaptation is the divergence of distribution between the target domain and source domain. Ben-David et al. [35, 36] defines a divergence measure $d_{H\Delta H}(S, T)$ between two domains S and T , which is widely used in the theory of nonconservative domain adaptation. Using this notion, they established a probabilistic bound on the performance $\epsilon_T(h)$ of some label classifier h from T evaluated on target domain given its performance $\epsilon_S(h)$ on the source domain. Formally,

$$\epsilon_T(h) \leq \epsilon_S(h) + \frac{1}{2}d_{H\Delta H}(S, T) + \lambda \quad (1)$$

where λ is supposed to be a negligible term and dose not depend on classifier h .

Eq. 1 tells us that to adapt well, one has to learn a label classifier h which works well on source domain while reducing the $d_{H\Delta H}(S, T)$ divergence between S and T . Estimating $d_{H\Delta H}(S, T)$ for a finite sample is exactly the problem of minimizing the empirical risk of a domain classifier h_d that discriminates between instances drawn from S and instances drawn from T , respectively pseudo-labeled with 0 and 1. More specifically, it involves the following steps:

1. Pseudo-labeling the source and target instances with 0 and 1, respectively.
2. Randomly sampling two sets of instances as the training and testing set.
3. Learning a domain classifier h_d on the training set and verifying its performance on the testing set.
4. Estimating the distance as $\hat{d}_{H\Delta H}(S, T) = 1 - 2\epsilon(h_d)$, where $\epsilon(h_d)$ is the test error.

It's obvious that if two domains perfectly overlap with each other, $\epsilon(h_d) \approx 0.5$, and $\hat{d}_{H\Delta H}(S, T) \approx 0$. On the contrary, if two domains are completely distinct from each other, $\epsilon(h_d) \approx 0$, and $\hat{d}_{H\Delta H}(S, T) \approx 1$. Therefore, $\hat{d}_{H\Delta H}(S, T) \in [0, 1]$. The lower the value is, the smaller two domains divergence.

This observation leads to our idea. We have to learn two classifiers (i.e. a label classifier h_l and a domain classifier h_d) using the feature representation f learned by a feature extractor. The parameters θ_l of h_l and θ_d of h_d should be optimized to minimize the label prediction loss $\epsilon_S(h_l)$ (for the source domain) and the domain classification loss $\epsilon(h_d)$ (for all domains). And the parameters θ_f of the feature extractor should be discriminative to minimize $\epsilon_S(h_l)$ and domain-invariant to minimize $1 - 2\epsilon(h_d)$.

3. Proposed adversarial adaptive CNN

3.1. Problem Formalization

Let the labeled source domain data as $D_S = \{(x_S^i, y_S^i)\}_{i=1}^{N_S}$, where $x_S^i \in \mathcal{R}^{m \times 1}$ is the data instance and $y_S^i \in \{1, \dots, K\}$ is the corresponding class label. While, $D_T = \{(x_T^i)\}_{i=1}^{N_T}$ is the unlabeled target domain data. Here, N_S and N_T are the numbers of instances in D_S and D_T . In addition, each data instance is pseudo-labeled with a domain label $d \in \{0, 1\}$ respectively, which indicates whether the instance comes from the source domain ($d = 0$) or from the target domain ($d = 1$).

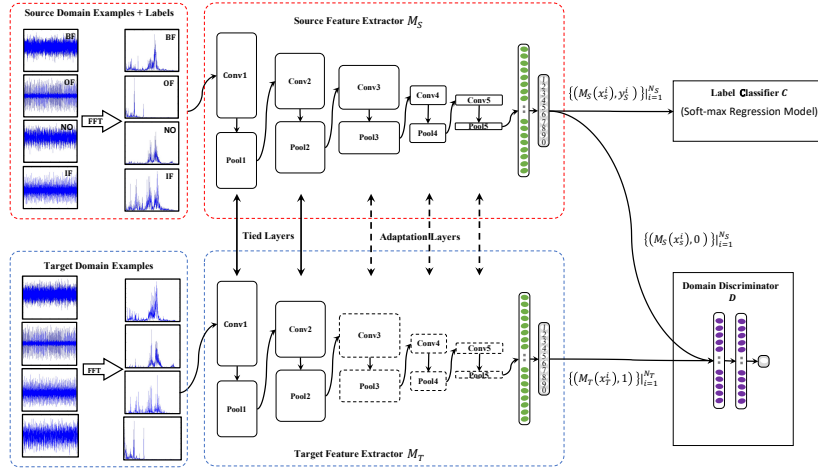


Figure 1: The proposed Adversarial Adaptive CNN (A2CNN) includes a source feature extractor M_S , a target feature extractor M_T , a label classifier C and a domain discriminator. Solid lines indicate tied layers, and Dashed lines indicate adaptive layers.

The overall framework of the proposed Adversarial Adaptive CNN (A2CNN) is shown in Figure 1. It includes a source feature extractor M_S , a target feature extractor M_T , a label classifier C and a domain discriminator D , which together form a deep feed-forward architecture that maps each input sample x_S^i (resp. x_T^i) to a K -dimensional feature vector $M_S(x_S^i)$ (resp. $M_T(x_T^i)$) (K equals to the number of class label) and predicts its class label $y \in \{1, \dots, K\}$ and its domain label $d \in \{0, 1\}$. Compared with the traditional deep domain adaptation models, the proposed framework is more like an adversarial learning framework.

Source feature extractor M_S . As shown in Figure 2, we compose the source feature extractor M_S from five 1-D convolutional layers and two fully-connected layers. The input of the first convolution layer (e.g., Conv 1) is the fast Fourier transform (FFT) spectrum amplitudes of vibration signals, which is the most widely used approach of bearing defect detection. The last fully-connected layer (e.g., FC 2) is called label layer [37] with an output of K neurons (equals to the number of class label), which is fed to label classifier C which estimate the posterior probability of each class. It is common to add a pooling layer after each convolution layer in the CNN architecture separately. It functions as a down-sampling operation which results in a reduced-resolution output feature map, which is robust to small variations in the location of features in the previous layer. The most commonly used pooling layer is max-pooling layer, which performs the local max operation over the input features. The main difference between the traditional 2-D and the 1-D CNN is the usage of 1-D arrays instead of 2-D matrices for both feature maps and filter kernels. In order to capture the useful information in the intermediate and low frequency bands, the wide kernels should be used in the first convolutional layer which can better suppress high frequency noise[23]. The following convolutional kernels are small (specifically, 3×1) which make the networks deeper to acquire good representations of the input signals and improve the performance of the network.

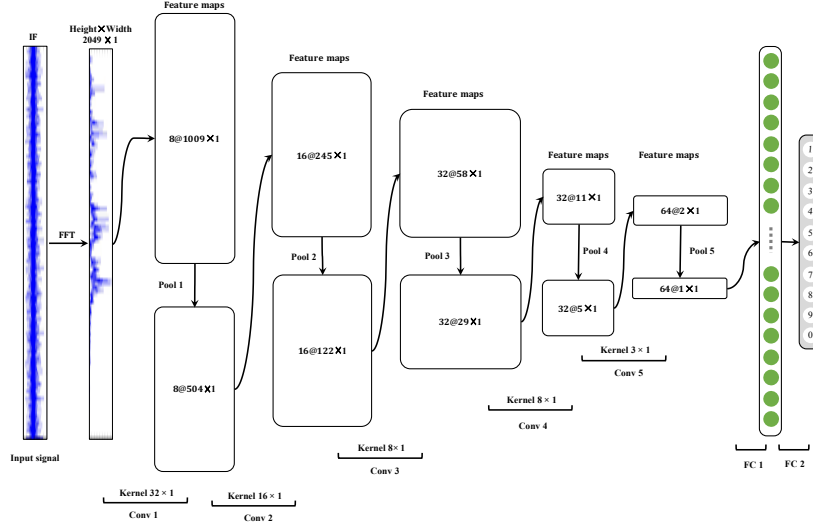


Figure 2: Structure of the source feature extractor M_S .

Label classifier C . For an source domain instance x_S^i , the output feature vector $M_S(x_S^i) \in \mathcal{R}^{K \times 1}$ mapped by the source feature extractor M_S is the input of the label classifier C . Here, the soft-max regression model [38] is used as the label classifier on source domain to incorporate label information. The soft-max regression model is a generalization of the logistic regression model for multi-class classification problems. We can estimate the probabilities of each class that x_S^i

belongs to as follows,

$$C(M_S(x_S^i)) = \begin{bmatrix} p(y=1|M_S(x_S^i)) \\ p(y=2|M_S(x_S^i)) \\ \vdots \\ p(y=K|M_S(x_S^i)) \end{bmatrix} = \frac{1}{\sum_{j=1}^K e^{u_j}} \begin{bmatrix} e^{u_1} \\ e^{u_2} \\ \vdots \\ e^{u_K} \end{bmatrix}, \text{ with } u_j = M_S(x_S^i)_j, \quad (2)$$

where u_j is the j -th value of $M_S(x_S^i)$, $\sum_{j=1}^K e^{u_j}$ is a normalized term, and $p(y=j|M_S(x_S^i))$ represent the distribution of the class $j \in \{1, 2, \dots, K\}$ given the input $M_S(x_S^i)$. Given the source domain data D_S , the parameters of the source feature extractor M_S can be derived by maximizing the following supervised loss,

$$\max_{M_S} L_{cls}(D_S) = \frac{1}{N_S} \sum_{i=1}^{N_S} \sum_{j=1}^K 1\{y_S^i = j\} [\log C(M_S(x_S^i))]. \quad (3)$$

where $1\{y_S^i = j\}$ is an indicator function, whose value is 1 if $y_S^i = j$, otherwise is 0.

Target feature extractor M_T . Based on "How to parametrize the target feature extractor", the approaches of most published adversarial adaptation works can be summarized into two categories: symmetric transformation and asymmetric transformation. For many prior symmetric transformation methods [39, 40], all layers are constrained, thus enforcing exact source and target mapping consistency. Although learning a symmetric transformation can reduce the number of parameters in the model, this may make the optimization poorly conditioned, since the same network must handle samples from two separate domains [41]. The intuitive idea behind the asymmetric transformation is to constrain a subset of the layers. Rozantsev et al. [42] showed that partially shared weights can lead to effective adaptation in both supervised and unsupervised settings. We choose to learn parameters of the target feature extractor M_T by partially untying layers between source and target mappings. As shown in Figure 1, solid lines indicate tied layers, and dashed lines indicate adaptive layers. Given that the target domain is unlabeled, we initialize the parameters of the target feature extractor M_T with the source feature extractor M_S .

Domain discriminator D . For an instance x_S^i (resp. x_T^i), the output feature vector $M_S(x_S^i)$ (resp. $M_T(x_T^i)$) mapped by the feature extractor M_S (resp. M_T), pseudo-labeled with a domain label $d^i = 0$ (resp. $d^i = 1$), is the input of the domain discriminator D . The domain discriminator D is a multi-layer perceptron (MLP), which is composed of several fully-connected layers (i.e. $input \rightarrow 500 \rightarrow 500 \rightarrow 1$). The domain discriminator is in the binary classification setting. With the logistic regression model, its loss takes the form below,

$$\max_D L_{adv_D} = \frac{1}{N_S} \sum_{i=1}^{N_S} [\log D(M_S(x_S^i))] + \frac{1}{N_T} \sum_{i=1}^{N_T} [\log(1 - D(M_T(x_T^i)))]. \quad (4)$$

In order to obtain domain-invariant features, we seek the parameters of the target feature extractor M_T to fool the domain discriminator D by maximizing the following loss function $L_{adv_{M_T}}$ with inverted domain labels [43],

$$\max_{M_T} L_{adv_{M_T}} = \frac{1}{N_T} \sum_{i=1}^{N_T} [\log D(M_T(x_T^i))]. \quad (5)$$

3.2. Model Learning

We have used two training steps to enhance the domain adaptation ability of our model. The details of the proposed algorithm is summarized in Algorithm 1.

Step 1: **Pre-train.** Train the source feature extractor M_S with labeled source training examples.

Step 2: **Adversarial adaptive fine tune.** Initialize the parameters of the target feature extractor M_T with the trained source feature extractor M_S and learn a target feature extractor M_T such that a domain discriminator D cannot predict the domain label of mapped source and target examples reliably.

3.3. Classifier Construction

After all the parameters are learned, we can construct classifier for the target domain in two ways. The first way is directly to use the output of the last fully connected layer of the target feature extractor M_T . That is, for any instance x_T^i in the target domain, the output of the target feature extractor $M_T(x_T^i)$ can computer the probability of instance x_T^i belonging to a label $j \in \{1, \dots, K\}$ using Eq. 2. We choose the maximum probability using Eq. 6. and the corresponding label as the prediction,

$$y_T^i = \max_j \frac{e^{u_j}}{\sum_{l=1}^K e^{u_l}}, \text{ with } u_j = M_T(x_T^i)_j. \quad (6)$$

The second way is to apply standard classification algorithms to train a classifier for source domain in the embedding space generated by the M_S . Then the classifier is applied to predict class labels for target domain data.

4. Experimental analysis of proposed A2CNN model

In real world applications, data under different load condition usually draw from different distribution. So it is significant to use unlabeled data under any load condition to rebuilt the classifier trained with samples collected in one load condition. In the reminder of this section, Case Western Reserve University (CWRU) bearing database [44] is used to investigate how well the proposed A2CNN method performs under this scenario.

4.1. Datasets and Preprocessing

The test-bed in CWRU Bearing Data Center is composed of a driving motor, a two hp motor for loading, a torque sensor/encoder, a power meter, accelerometers and electronic control unit. The test bearings locate in the motor shaft. Subjected to electrosparking, inner-race faults (IF), outer-race faults (OF) and ball fault (BF) with different sizes (0.007in, 0.014in, 0.021in and 0.028in) are introduced into the drive-end bearing of motor. The vibration signals are sampled by the accelerometers attached to the rack with magnetic bases under the sampling frequency of 12kHz. The experimental scheme simulates three working conditions with different motor load and rotating speed, i.e., Load1 = 1hp/1772rpm, Load2 = 2hp/1750rpm and Load3 = 3hp/1730rpm. The vibration signals of normal bearings (NO) under each working condition are also gathered.

In this paper, a vibration signal with length 4096 is randomly selected from raw vibration signal. Then, fast Fourier transform (FFT) is implemented on each signal and the 4096 Fourier

Algorithm 1 Adversarial Adaptive CNN (A2CNN)

- 1: **procedure** STEP1
- 2: **Input:** Given one source domain $D_S = \{(x_S^i, y_S^i)\}_{i=1}^{N_S}$.
- 3: **Output:** The parameters in the source feature extractor M_S .
- 4: **for** number of training iterations **do**
- 5: Sample minibatch of m instances $\{(x_S^1, y_S^1), \dots, (x_S^m, y_S^m)\}$ from the source domain D_S .
- 6: Update the domain discriminator M_S by ascending its stochastic gradient:

$$\nabla_{M_S} \frac{1}{m} \sum_{i=1}^m \sum_{j=1}^K 1\{y_S^i = j\} [\log C(M_S(x_S^i))].$$

- 7: **end for**
- 8: **end procedure**
- 9: **procedure** STEP2
- 10: **Input:** Given one source domain $D_S = \{(x_S^i, y_S^i)\}_{i=1}^{N_S}$, and one target domain $D_T = \{(x_T^i)\}_{i=1}^{N_T}$. The parameters in the source feature extractor M_S . The number of adaptive layers, l . The number of steps to apply to the discriminator, k .
- 11: **Output:** Results of the feature vector mapped by M_T , i.e., $\{M_T(x_T^i)\}_{i=1}^{N_T}$.
- 12: Initialize the parameters of the target feature extractor M_T with the source feature extractor M_S .
- 13: **for** number of training iterations **do**
- 14: **for** $i \leftarrow 1, k$ **do**
- 15: Sample minibatch of m instances $\{x_S^1, \dots, x_S^m\}$ from the source domain D_S .
- 16: Sample minibatch of m instances $\{x_T^1, \dots, x_T^m\}$ from the target domain D_T .
- 17: Update the domain discriminator D by ascending its stochastic gradient:

$$\nabla_D \frac{1}{m} \sum_{i=1}^m [\log D(M_S(x_S^i)) + \log(1 - D(M_T(x_T^i)))].$$

- 18: **end for**
- 19: Sample minibatch of m instances $\{x_T^1, \dots, x_T^m\}$ from the target domain D_T .
- 20: Update the final l adaptive layers of the target feature extractor M_T by ascending its stochastic gradient:

$$\nabla_{M_T} \frac{1}{m} \sum_{i=1}^m [\log D(M_T(x_T^i))].$$

- 21: **end for**
 - 22: **for** $j \leftarrow 1, N_T$ **do**
 - 23: Computing the $M_T(x_T^j)$.
 - 24: **end for**
 - 25: **end procedure**
-

coefficients are generated. Since the coefficients are symmetric, the first 2048 coefficients are used in each sample. The samples collected from the above three different conditions form three domains, namely A, B and C, respectively. There are ten classes under each working condition, including nine kinds of faults and a normal state, and each class consists of 800 training samples and 800 testing samples. Therefore, each domain contains 8000 training samples and 8000 testing samples of ten classes collected from corresponding working condition. The details of all domains are described in Table 1.

Table 1: Description of rolling element bearing domains

Fault location		None	IF	BF				OF				Load
Category labels		1	2	3	4	5	6	7	8	9	10	
Fault diameter (in.)		0	0.007	0.014	0.021	0.007	0.014	0.021	0.007	0.014	0.021	
Domain A	Train	800	800	800	800	800	800	800	800	800	800	1
	Test	800	800	800	800	800	800	800	800	800	800	1
Domain B	Train	800	800	800	800	800	800	800	800	800	800	2
	Test	800	800	800	800	800	800	800	800	800	800	2
Domain C	Train	800	800	800	800	800	800	800	800	800	800	3
	Test	800	800	800	800	800	800	800	800	800	800	3

The description of scenario settings for domain adaptation is illustrated in Table 2.

Table 2: Description of scenario settings for load domain adaptation.

Scenario settings for load domain adaptation			
Domain types	Source domain	Target domain	
Description	Labeled signals under one single load	Unlabeled signals under another load	
Domain details	Training set in domain A	Test set in domain B	Test set in domain C
	Training set in domain B	Test set in domain A	Test set in domain C
	Training set in domain C	Test set in domain A	Test set in domain B

4.2. Experimental setup

4.2.1. Baseline Methods

We compare our methods with the following baselines,

1. Traditional SVM and Multi-layer Perceptron (MLP) which work with the data transformed by Fast Fourier transformation (FFT).
2. The deep neural network (DNN) system [10] with frequency features proposed by Lei et al. in 2016. The DNN system has two steps, namely, pre-training with unsupervised stacked auto-encoder and supervised fine tuning. This neural network consists of three hidden layers. The number of neurons in each layer is 1025, 500, 200, 100 and 10. The input of the network is the normalized 1025 Fourier coefficients transformed from the raw temporal signals using FFT. Soft-max is used as the classifier for supervised learning.
3. The Deep Convolution Neural Networks with Wide first-layer kernels (WDCNN) system proposed by Zhang et al. in 2017. The WDCNN system works directly on raw temporal signals. It contains five convolutional layers. Batch Normalization (BN) layers with statistical information of the target domain are implemented right after the convolutional layers and the fully-connected layer to accelerate the training process and improve the robustness of the system to the change of working condition. The domain adaptation capacity of this model originates in the domain adaptation method named Adaptive Batch Normalization (AdaBN).

4.2.2. Parameters of the proposed A2CNN

The feature extractor M_S and M_T used in experiments is composed of five convolutional layers and pooling layers followed by two fully-connected hidden layers. The pooling type is max pooling and the activation function is ReLU. The parameters of the convolutional and pooling layers are detailed in Table 3. In order to minimize the loss function, the Adam Stochastic optimization algorithm is applied to train our CNN model. The final l ($l \in [1, 5]$) layers of the target feature extractor M_T is untied and used as adaptive layers. The domain discriminator D consist of three fully-connected layers. The number of neurons in each layer is 500, 500 and 1. The experiments were implemented using Tensorflow toolbox of Google.

Table 3: Details of proposed A2CNN model used in experiments.

No.	Layer type	Kernel size	stride	Kernel channel size	Output size (width * depth)	Padding
1	Convolution1	32×1	2×1	8	1009×8	Yes
2	Pooling1	2×1	2×1	8	504×8	No
3	Convolution2	16×1	2×1	16	245×16	Yes
4	Pooling2	2×1	2×1	16	122×16	No
5	Convolution3	8×1	2×1	32	58×32	Yes
6	Pooling3	2×1	2×1	32	29×32	No
7	Convolution4	8×1	2×1	32	11×32	Yes
8	Pooling4	2×1	2×1	32	5×32	No
9	Convolution5	3×1	2×1	64	2×64	Yes
10	Pooling5	2×1	2×1	64	1×64	No
11	Fully-connected	500		1	500	
12	Fully-connected	10		1	10	

By contrast, for an instance from the target domain x_T^i , in order to investigate the effectiveness of adversarial adaptation, we use the corresponding output of the well-trained source feature extractor $M_S(x_T^i)$ to compute the probability of the instance x_T^i belonging to a label $j \in \{1, \dots, K\}$ using Eq. 2, which is denoted as $A2CNN_S$.

4.3. Accuracy across different domains

As Figure 3 shows, SVM, MLP and DNN perform poorly in domain adaptation, with average accuracy in the six scenarios being around 65%, 80% and 80%. Which prove that samples under different working conditions draw from the different distributions and models trained under one working condition is not suitable for fault classification under another working load condition.

Compared with the WDCNN with AdaBN, which achieved the state-of-art domain adaptation ability, A2CNN which achieves 99.21% accuracy in average is obviously greater than WDCNN (AdaBN) with average accuracy being 95.95%. This result prove that the features learned by A2CNN are more domain invariant than the features learned by the other methods.

In addition, by comparing A2CNN with $A2CNN_S$, we can find that in every scenario, the performance of A2CNN is superior to $A2CNN_S$. This means that the adversarial adaptation training can significantly improve the bearing fault diagnosis under varying working conditions.

It is also interesting that when adapting from Domain A to B, from B to A, from B to C, and from C to B, the fault diagnosis accuracy of the proposed A2CNN is only a bit better than WDCNN (AdaBN). However, when adapting from domain A to C and C to A, the proposed A2CNN is significantly better than the other methods. This result prove that A2CNN is good at solving the problem that the distributions of source domain and target domain are far different.

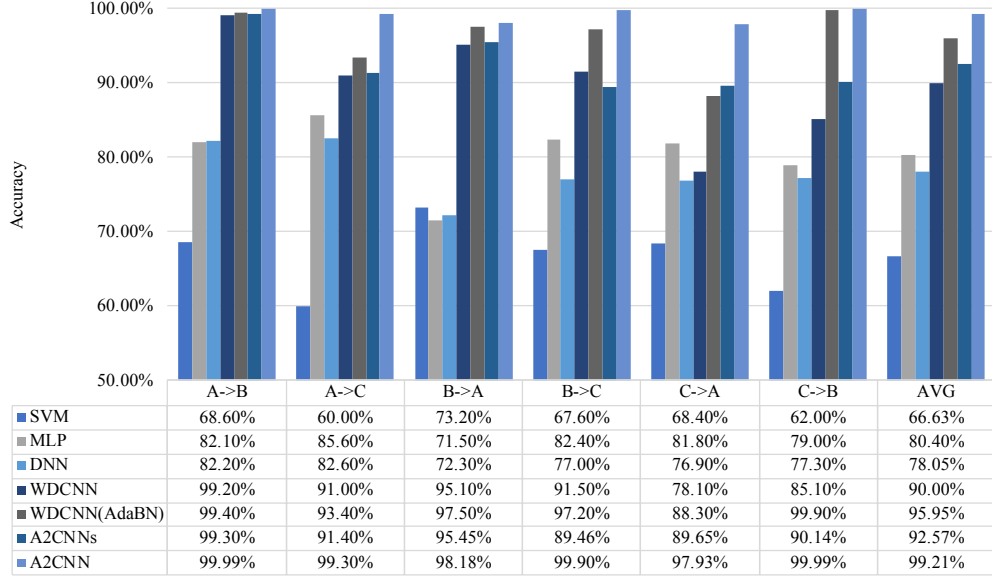


Figure 3: Accuracy (%) on six domain adaptation problems.

4.4. Sensitivity Analysis of Faults

For each type of fault detection, in order to further analyze the sensitivity of the proposed A2CNN model, we introduce two new evaluation indicator, i.e. *precision* and *recall*, which are widely used in pattern recognition, information retrieval and binary classification.

In the fault diagnosis context, the *precision* and *recall* for a kind of fault type f (e.g. inner fault) can be calculated as below,

$$precision(f) = \frac{faults\ f\ correctly\ identified}{faults\ f\ correctly\ identified + other\ instances\ incorrectly\ labeled\ as\ f} \quad (7)$$

$$recall(f) = \frac{fault\ f\ correctly\ identified}{faults\ f\ correctly\ identified + faults\ f\ incorrectly\ labeled\ as\ not\ f} \quad (8)$$

A *precision* score of 1.0 for a fault type f means that every sample labeled as belonging to class f does indeed belong to class f (i.e. there is no false alarm), but it can't tell us about the number of samples from class f that were not labeled correctly (i.e. how many failures are missing?).

Whereas a *recall* of 1.0 means that every item from a fault type f was labeled as belonging to class f (i.e. there is no missing alarm), but says nothing about how many other items were incorrectly also labeled as belonging to class f (i.e. how many false alarms are there?).

The *precision* and *recall* of every class processed by A2CNN and A2CNN_s are detailed in Table 4 and Table 5.

In Table 4, for the 3rd kinds of fault (i.e. IF with fault size being 0.014 in.), A2CNN_s has low precision when adapting from domain B to C and from C to A, which are 49.63% and 57.55% respectively. This means that about half of that kind of fault alarms are unreliable.

Meanwhile, In Table 5, for the 2nd kinds of fault (i.e. IF with fault size being 0.007 in.), A2CNN_S has very low recall when adapting from domain B to C and from C to A, which are 1.13% and 26.75% respectively. This means that about a large number of that kind of failures are not detected.

In general, the *precision* and *recall* of A2CNN are higher than that of A2CNN_S, which implies that A2CNN has fewer false alarms (i.e. high *precision* score) and missed alarms (i.e. high *recall* score). We can find that A2CNN can make almost all class classified into right class, except BF with fault size being 0.014 in and BF with fault size being 0.021 in.

This result shows that after adversarial training, the classification performance on every class achieve remarkable improvement.

Table 4: *precision* of the proposed A2CNN_S and A2CNN on six domain adaptation problems.

Fault location	None	IF				BF				OF		
Fault diameter (in.)		0.007	0.014	0.021		0.007	0.014	0.021		0.007	0.014	0.021
Category labels	1	2	3	4		5	6	7		8	9	10
<i>precision of A2CNN_S</i>												
A→B	100%	100%	100%	100%		100%	100%	98.64%		100%	100%	100%
A→C	92.27%	100%	100%	100%		99.75%	92.82%	99.46%		100%	100%	100%
B→A	100%	100%	100%	100%		87.43%	93.68%	100%		100%	100%	100%
B→C	96.74%	100%	49.63%	100%		100%	99.49%	100%		100%	100%	100%
C→A	100%	100%	57.55%	100%		83.33%	95.40%	100%		95.12%	100%	100%
C→B	100%	100%	93.13%	99.88%		98.89%	100%	100%		100%	100%	100%
<i>precision of A2CNN</i>												
A→B	100%	100%	100%	100%		100%	100%	99.88%		100%	100%	100%
A→C	93.46%	100%	100%	100%		100%	100%	100%		100%	100%	100%
B→A	100%	100%	100%	100%		90.70%	92.59%	100%		100%	100%	100%
B→C	100%	100%	99.01%	100%		100%	100%	100%		100%	100%	100%
C→A	100%	100%	100%	100%		90.91%	90.40%	100%		100%	100%	100%
C→B	100%	100%	100%	100%		99.88%	100%	100%		100%	100%	100%

Table 5: *recall* of the proposed A2CNN_S and A2CNN on six domain adaptation problems.

Fault location	None	IF	BF				OF			
Fault diameter (in.)		0.007	0.014	0.021	0.007	0.014	0.021	0.007	0.014	0.021
Category labels	1	2	3	4	5	6	7	8	9	10
<i>recall of A2CNN_S</i>										
A→B	100%	100%	100%	100%	98.63%	100%	100%	100%	100%	100%
A→C	100%	100%	99.75%	100%	99.50%	92.13%	92.88%	100%	99.50%	100%
B→A	100%	100%	100%	100%	100%	100%	81.75%	100%	100%	100%
B→C	100%	1.13%	100%	100%	100%	96.63%	99.50%	100%	97.38%	100%
C→A	100%	26.75%	100%	100%	100%	96.00%	73.75%	100%	100%	100%
C→B	100%	92.63%	100%	100%	100%	99.88%	98.88%	100%	100%	100%
<i>recall of A2CNN</i>										
A→B	100%	100%	100%	100%	100%	99.88%	100%	100%	100%	100%
A→C	100%	100%	100%	100%	100%	93.00%	100%	100%	100%	100%
B→A	100%	100%	100%	100%	100%	100%	78.88%	100%	100%	100%
B→C	100%	100%	100%	100%	100%	100%	100%	100%	99.00%	100%
C→A	100%	100%	100%	100%	100%	100%	79.38%	100%	100%	100%
C→B	100%	100%	100%	100%	100%	100%	99.88%	100%	100%	100%

4.5. Networks visualizations

Generally, deep learning is an empirical success rather than a mathematical solution to the learning problem. For explaining why A2CNN can have high domain adaptation capacity and

have a great performance in bearing fault diagnosis vividly, the learned features of A2CNN and the changes of feature distribution of the samples from source domain and target domain extracted by A2CNN during the training stage are visualized in this subsection. t-Distributed Stochastic Neighbor Embedding (t-SNE) is a technique for dimensionality reduction that is particularly well suited for the visualization of high-dimensional datasets. The goal of t-SNE is to take a set of points in a high-dimensional space and find a faithful representation of those points in a lower-dimensional space, typically the 2D plane. In this paper, t-SNE is used to visualize the features extracted by A2CNN. For more details about t-SNE one can refer to Ref.[45].

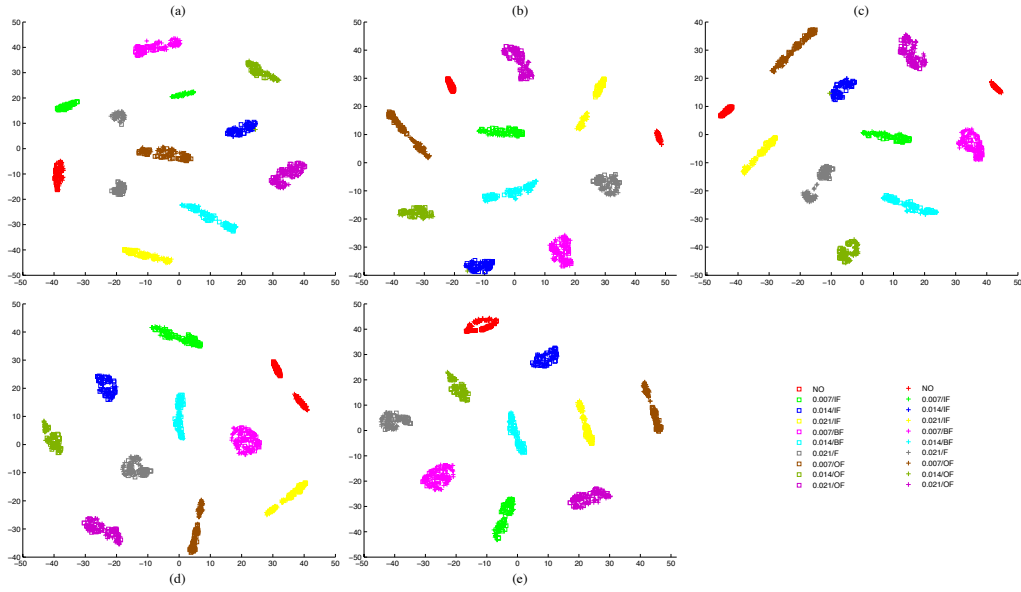
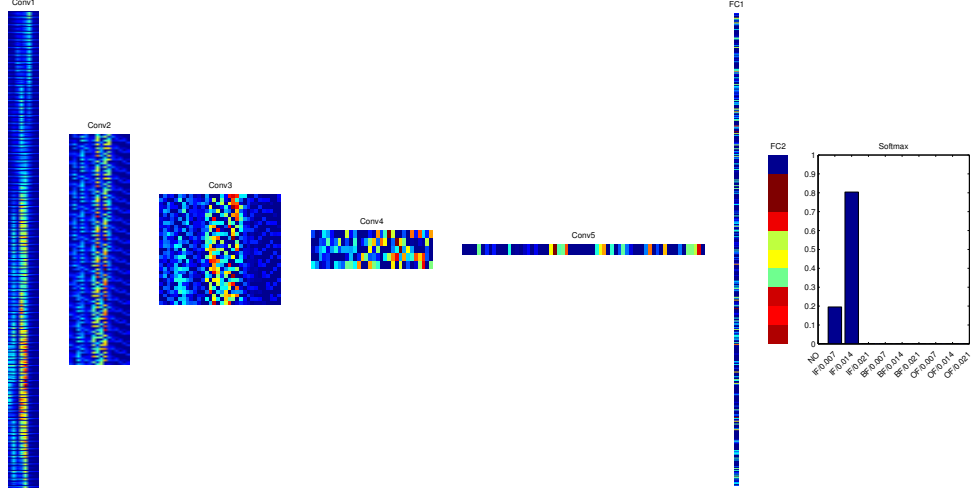
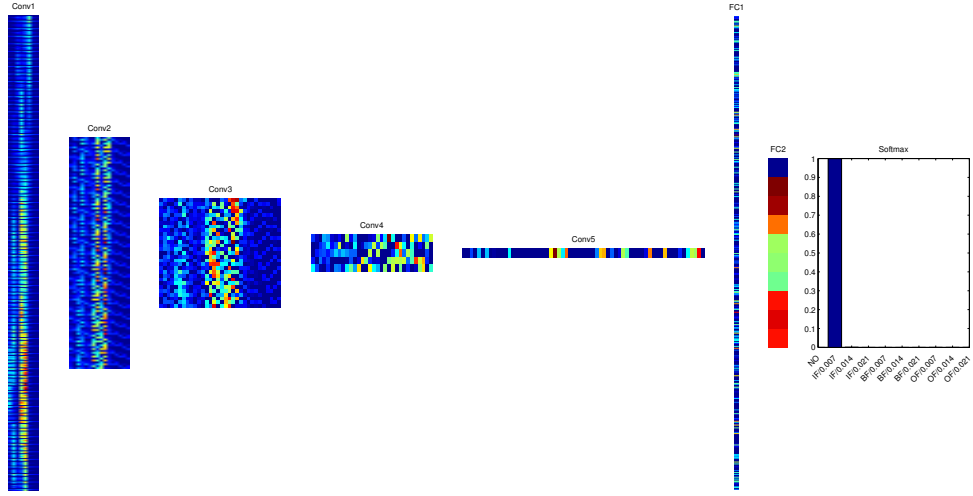


Figure 4: Visualization of feature distribution of samples from source domain and target domain via t-SNE: (a) features are extracted by the last full-connected layer of trained source CNN. features are extracted by the last full-connected layer of target CNN, with 500, 1000, 1500 and 2000 iterations respectively in (b),(c),(d) and (e). Square symbols and cross symbols represent data from source domain (Load2) and data from target domain (Load3) respectively. The ten different faults are shown by ten different colors.

Take the domain adaption task $B \rightarrow C$ as an example, t-SNE is used to visualize high-dimensional features extracted by the last full-connected layer of trained source CNN and target CNN, with 500, 1000, 1500 and 2000 iterations. The result is shown in Figure4 and there are some interesting phenomena worth noticing. Firstly, whatever the features are extracted by source CNN or target CNN, the features are all divisible. It is obvious that CNN with five convolution layers has qualifications for classifying the faults of bearing in this experiment. Second, in Figure4(a), distributions of features of data under Load2 and Load3 extracted by the full-connected layer of trained source CNN are different. Ball faults 0.021 in under Load2 condition are not similar with ball faults 0.021 in under Load3 condition based on the probability. Also,



(a) 3-1-803



(b) 3-1-1-803

Figure 5: Visualization of all convolutional neuron activations of (a) source CNN when IF with 0.014 in fault diameter under Load2 is taken as input. (b) Source CNN when IF with 0.014 in fault diameter under Load3 is taken as input and (c) Target CNN when IF with 0.014 in fault diameter under Load3 is taken as input.

inner faults 0.007 in under Load2 condition are not similar with inner faults 0.007 in under Load3 condition. Actually when we use these features classify the faults of bearing, the classification error rates of inner faults 0.007 in and ball faults 0.021 in are 0.011 and 0.995 respectively. The results are some kind of coincident with the result shown in Figure4(a) because t-SNE shows

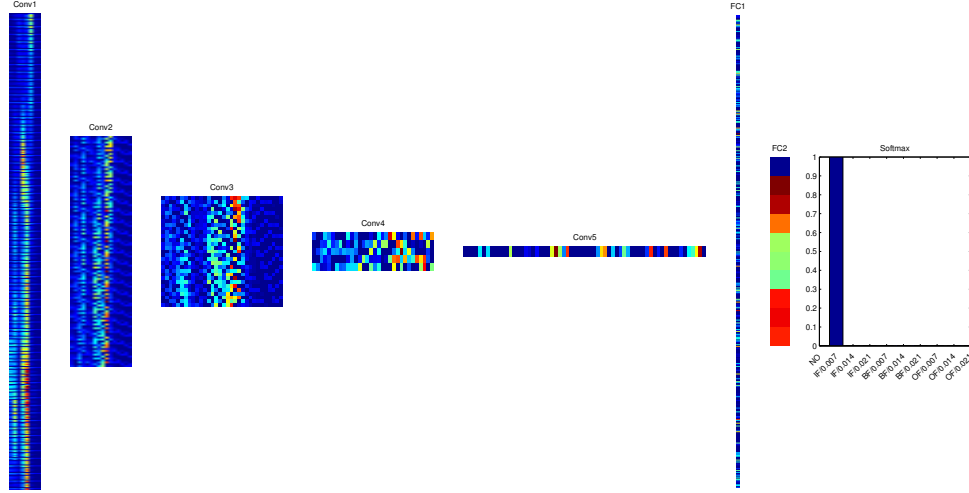


Figure 6: 3-3-803

the similarity in probability, which is different from the classification rule of the classifier we used, softmax layer. Which prove that the model trained on one certain load condition cannot always be directly applied on another load condition because data distribution always changes with the load varying. Lastly, with the number of adversarial iterations increase, the distributions of features of data under Load2 and Load3 extracted by the full-connected layer of trained source CNN are becoming more and more similar. When the features extracted by target CNN with 500, 1000, 1500, 2000 adversarial iterations are applied to classify faults of bearing, the classification accuracies are 0.9949, 0.9975, 0.9981 and 0.9990 respectively. The features can be used to classify the faults under Load3 condition. The phenomenon indicates that the adversarial network is effective and A2CNN has strong domain adaptation capacity.

Secondly, we visualize the reactions of neurons of all the convolutional layers and full-connected layer to display what each layer learn in A2CNN. The inner race faults with 0.014 in fault diameter under Load2 and Load3 are chosen as the input of source CNN respectively and the reactions of neurons of source CNN in these two experiment are shown in Figure 5(a) and Figure 5(b). Figure 5(c) shows the reactions of neurons of A2CNN, when the inner race faults with 0.014-inch fault diameter under Load3 is fed into A2CNN. The source CNN is trained under Load3 and the A2CNN is the source CNN after adversarial train under Load3. We can find that compared to source CNN, A2CNN use more neurons to describe the inner race faults with 0.014-inch fault diameter under Load3. Otherwise, the way A2CNN describe the inner race faults with 0.014-inch fault diameter under Load3 is similar with the way source CNN trained under Load2 describe the inner race faults with 0.014-inch fault diameter under Load2. The phenomenon is especially obvious in the third convolution layer. As Figure 5(b) shows, when taking the inner race faults with 0.014-inch fault diameter under Load3 as the input of source CNN, the output of neurons in the left side of Conv3 activations are almost zeros which is seriously different from the Conv3 activations in Figure 5(a). The above difference result in the wrong classification that

the inner race faults with 0.014-inch fault diameter is classified into the inner race faults with 0.021-inch fault diameter. However after the adversarial train, neurons in the left side of Conv3 activations of A2CNN are active like the Conv3 activations of source CNN in Figure 5(a). This proves that the A2CNN network can learn the difference between domains under two different load condition and the features extracted by A2CNN have high domain adaptation ability.

5. Conclusion

This paper proposes a new model named A2CNN, to address the fault diagnosis under varying working condition. A2CNN apply generative adversarial networks into bearing fault diagnosis, which is the first attempt in bearing fault diagnosis and perform well. Transfer learning based on parameters is also applied into the training of A2CNN. The initial parameters of target CNN are transferred from source CNN trained under source CNN.

Results in Section 4 shows that, although state of the art DNN model could achieve pretty high accuracy on normal dataset, its performance suffer from rapid degradation when working load changes. There are some domain adaptation based on CNN addressing the fault diagnosis under varying working condition and acquire some achievement. However, when the load changes a lot, these methods degrade dramatically. Apparently, the proposed A2CNN is robust to more working conditions. In Section 4, feature visualization of A2CNN via t-SNE and networks visualization are used to investigate the inner mechanism of the proposed A2CNN model.

The proposed A2CNN still has room for improvement. In the future work, we can try to introduce ensemble learning to improve the stability and accuracy of the algorithm because ensemble learning is to combine kinds of weak classifiers to get a strong classifier. The strong classifier is more stable than other weak classifiers. Results in Section 4 shows that, the greater the change in working conditions, the worse the classification, which is kind of unstable. So introducing ensemble learning into the proposed A2CNN is worth studying.

References

References

- [1] G. J. Vachtsevanos, F. Lewis, A. Hess, B. Wu, Intelligent fault diagnosis and prognosis for engineering systems, Wiley Online Library, 2006.
- [2] Z. Qiao, Y. Lei, J. Lin, F. Jia, An adaptive unsaturated bistable stochastic resonance method and its application in mechanical fault diagnosis, *Mechanical Systems and Signal Processing* 84 (2017) 731–746.
- [3] P. Albrecht, J. Appiarius, E. Cornell, D. Houghtaling, R. McCoy, E. Owen, D. Sharma, Assessment of the reliability of motors in utility applications, *IEEE Transactions on Energy Conversion EC-2* (3) (1987) 396–406. doi:10.1109/TEC.1987.4765865.
- [4] A. K. S. Jardine, D. Lin, D. Banjevic, A review on machinery diagnostics and prognostics implementing condition-based maintenance, *MECHANICAL SYSTEMS AND SIGNAL PROCESSING* 20 (7) (2006) 1483–1510. doi: {10.1016/j.ymssp.2005.09.012}.
- [5] L. Ya-Guo, H. Zheng-Jia, Advances in applications of hybrid intelligent fault diagnosis and prognosis technique [j], *Journal of Vibration and Shock* 9 (2011) 030.
- [6] K. He, G. Gkioxari, P. Dollár, R. Girshick, Mask r-cnn, in: *Computer Vision (ICCV)*, 2017 IEEE International Conference on, IEEE, 2017, pp. 2980–2988.
- [7] L.-C. Chen, G. Papandreou, I. Kokkinos, K. Murphy, A. L. Yuille, Deeplab: Semantic image segmentation with deep convolutional nets, atrous convolution, and fully connected crfs, *IEEE transactions on pattern analysis and machine intelligence* 40 (4) (2018) 834–848.
- [8] W. Xiong, J. Droppo, X. Huang, F. Seide, M. Seltzer, A. Stolcke, D. Yu, G. Zweig, The microsoft 2016 conversational speech recognition system, in: *Acoustics, Speech and Signal Processing (ICASSP)*, 2017 IEEE International Conference on, IEEE, 2017, pp. 5255–5259.

- [9] Y. Zhang, W. Chan, N. Jaitly, Very deep convolutional networks for end-to-end speech recognition, in: *Acoustics, Speech and Signal Processing (ICASSP)*, 2017 IEEE International Conference on, IEEE, 2017, pp. 4845–4849.
- [10] F. Jia, Y. Lei, J. Lin, X. Zhou, N. Lu, Deep neural networks: A promising tool for fault characteristic mining and intelligent diagnosis of rotating machinery with massive data, *Mechanical Systems and Signal Processing* 72 (2016) 303–315. doi:<http://dx.doi.org/10.1016/j.ymssp.2015.10.025>.
- [11] Z. Huijie, R. Ting, W. Xinqing, Z. You, F. Husheng, Fault diagnosis of hydraulic pump based on stacked autoencoders, in: *Electronic Measurement & Instruments (ICEMI)*, 2015 12th IEEE International Conference on, Vol. 1, IEEE, 2015, pp. 58–62.
- [12] L. Guo, H. Gao, H. Huang, X. He, S. Li, Multifeatures fusion and nonlinear dimension reduction for intelligent bearing condition monitoring, *Shock and Vibration* 2016.
- [13] N. K. Verma, V. K. Gupta, M. Sharma, R. K. Sevakula, Intelligent condition based monitoring of rotating machines using sparse auto-encoders, in: *Prognostics and Health Management (PHM)*, 2013 IEEE Conference on, IEEE, 2013, pp. 1–7.
- [14] F. AlThobiani, A. Ball, et al., An approach to fault diagnosis of reciprocating compressor valves using teager–kaiser energy operator and deep belief networks, *Expert Systems with Applications* 41 (9) (2014) 4113–4122.
- [15] M. Gan, C. Wang, et al., Construction of hierarchical diagnosis network based on deep learning and its application in the fault pattern recognition of rolling element bearings, *Mechanical Systems and Signal Processing* 72 (2016) 92–104.
- [16] J. Tao, Y. Liu, D. Yang, Bearing fault diagnosis based on deep belief network and multisensor information fusion, *Shock and Vibration* 2016.
- [17] A. Krizhevsky, I. Sutskever, G. E. Hinton, Imagenet classification with deep convolutional neural networks, in: *Advances in neural information processing systems*, 2012, pp. 1097–1105.
- [18] Y. LeCun, L. Bottou, Y. Bengio, P. Haffner, Gradient-based learning applied to document recognition, *Proceedings of the IEEE* 86 (11) (1998) 2278–2324.
- [19] K. Simonyan, A. Zisserman, Very deep convolutional networks for large-scale image recognition, *arXiv preprint arXiv:1409.1556*.
- [20] K. He, X. Zhang, S. Ren, J. Sun, Deep residual learning for image recognition, in: *Proceedings of the IEEE conference on computer vision and pattern recognition*, 2016, pp. 770–778.
- [21] C. Szegedy, S. Ioffe, V. Vanhoucke, A. A. Alemi, Inception-v4, inception-resnet and the impact of residual connections on learning., in: *AAAI*, 2017, pp. 4278–4284.
- [22] T. Ince, S. Kiranyaz, L. Eren, M. Askar, M. Gabbouj, Real-time motor fault detection by 1-d convolutional neural networks, *IEEE Transactions on Industrial Electronics* 63 (11) (2016) 7067–7075.
- [23] W. Zhang, G. Peng, C. Li, Y. Chen, Z. Zhang, A new deep learning model for fault diagnosis with good anti-noise and domain adaptation ability on raw vibration signals, *Sensors (Basel, Switzerland)* 17 (2) (2017) 425.
- [24] X. Guo, L. Chen, C. Shen, Hierarchical adaptive deep convolution neural network and its application to bearing fault diagnosis, *Measurement* 93 (2016) 490–502.
- [25] F. Shen, C. Chen, R. Yan, R. X. Gao, Bearing fault diagnosis based on svd feature extraction and transfer learning classification, in: *Prognostics and System Health Management Conference (PHM)*, 2015, IEEE, 2015, pp. 1–6.
- [26] W. Lu, B. Liang, Y. Cheng, D. Meng, J. Yang, T. Zhang, Deep model based domain adaptation for fault diagnosis, *IEEE Transactions on Industrial Electronics* 64 (3) (2017) 2296–2305.
- [27] G.-S. Xie, X.-Y. Zhang, S. Yan, C.-L. Liu, Hybrid cnn and dictionary-based models for scene recognition and domain adaptation, *IEEE Transactions on Circuits and Systems for Video Technology* 27 (6) (2017) 1263–1274.
- [28] W. Zhang, C. Li, G. Peng, Y. Chen, Z. Zhang, A deep convolutional neural network with new training methods for bearing fault diagnosis under noisy environment and different working load, *Mechanical Systems and Signal Processing* 100 (2018) 439–453.
- [29] I. Goodfellow, J. Pouget-Abadie, M. Mirza, B. Xu, D. Warde-Farley, S. Ozair, A. Courville, Y. Bengio, Generative adversarial nets, in: *Advances in neural information processing systems*, 2014, pp. 2672–2680.
- [30] S. J. Pan, Q. Yang, A survey on transfer learning, *IEEE Transactions on Knowledge and Data Engineering* 22 (10) (2010) 1345–1359.
- [31] H. Shimodaira, Improving predictive inference under covariate shift by weighting the log-likelihood function, *Journal of Statistical Planning and Inference* 90 (2) (2000) 227–244.
- [32] M. Sugiyama, T. Suzuki, S. Nakajima, H. Kashima, P. von Büna, M. Kawanabe, Direct importance estimation for covariate shift adaptation, *Annals of the Institute of Statistical Mathematics* 60 (4) (2008) 699–746.
- [33] J. Huang, A. J. Smola, A. Gretton, K. M. Borgwardt, B. Scholkopf, Correcting sample selection bias by unlabeled data, in: *Proceedings of the 19th International Conference on Neural Information Processing Systems*, MIT Press, Cambridge, MA, USA, 2006, pp. 601–608.
- [34] B. Zadrozny, Learning and evaluating classifiers under sample selection bias, in: *Proceedings of the 21st International Conference on Machine Learning*, ACM, New York, NY, USA, 2004, pp. 114–122.
- [35] S. Ben-David, J. Blitzer, K. Crammer, A. Kulesza, F. Pereira, J. W. Vaughan, A theory of learning from different

- domains, *Machine Learning* 79 (1) (2010) 151–175. doi:{10.1007/s10994-009-5152-4}.
- [36] S. Ben-David, J. Blitzer, K. Crammer, F. Pereira, Analysis of representations for domain adaptation, in: *Proceedings of the 19th International Conference on Neural Information Processing Systems, NIPS'06*, MIT Press, Cambridge, MA, USA, 2006, pp. 137–144.
 - [37] F. Zhuang, X. Cheng, P. Luo, S. J. Pan, Q. He, Supervised representation learning: Transfer learning with deep autoencoders, in: *Proceedings of the 24th International Conference on Artificial Intelligence, IJCAI'15*, AAAI Press, 2015, pp. 4119–4125.
 - [38] J. Friedman, T. Hastie, R. Tibshirani, Regularization paths for generalized linear models via coordinate descent, *Journal of Statistical Software, Articles* 33 (1) (2010) 1–22.
 - [39] Y. Ganin, V. S. Lempitsky, Unsupervised domain adaptation by backpropagation., in: F. R. Bach, D. M. Blei (Eds.), *ICML*, Vol. 37 of *JMLR Workshop and Conference Proceedings*, JMLR.org, 2015, pp. 1180–1189.
 - [40] E. Tzeng, J. Hoffman, T. Darrell, K. Saenko, Simultaneous deep transfer across domains and tasks, *CoRR abs/1510.02192*. [arXiv:1510.02192](https://arxiv.org/abs/1510.02192).
URL <http://arxiv.org/abs/1510.02192>
 - [41] E. Tzeng, J. Hoffman, K. Saenko, T. Darrell, Adversarial discriminative domain adaptation, in: *Proceedings of the 2017 IEEE Conference on Computer Vision and Pattern Recognition, CVPR'17*, 2017, pp. 2962–2971.
 - [42] A. Rozantsev, M. Salzmann, P. Fua, Beyond sharing weights for deep domain adaptation, *CoRR abs/1603.06432*. [arXiv:1603.06432](https://arxiv.org/abs/1603.06432).
URL <http://arxiv.org/abs/1603.06432>
 - [43] I. J. Goodfellow, J. Pouget-Abadie, M. Mirza, B. Xu, D. Warde-Farley, S. Ozair, A. C. Courville, Y. Bengio, Generative adversarial nets, in: *Advances in Neural Information Processing Systems 27: Annual Conference on Neural Information Processing Systems 2014, December 8-13 2014, Montreal, Quebec, Canada, 2014*, pp. 2672–2680.
URL <http://papers.nips.cc/paper/5423-generative-adversarial-nets>
 - [44] Case western reserve university bearings vibration dataset available: <http://csegroups.case.edu/bearingdatacenter/home>.
 - [45] A. Prezgonzlez, M. Vergara, J. L. Sanchobru, L. J. P. Van, Der Maaten, G. E. Hinton, D. Shanmugapriya, G. Padmavathi, J. Kubo, P. E. E. Gantz, I. Science, Visualizing data using t-sne, *Journal of Machine Learning Research* 9 (2605) (2008) 2579–2605.